



# HHS Public Access

Author manuscript

*Nat Commun.* Author manuscript; available in PMC 2015 August 05.

Published in final edited form as:

*Nat Commun.* ; 6: 6219. doi:10.1038/ncomms7219.

## Imaging regulatory T cell dynamics and suppression of T cell priming mediated by CTLA4

Melanie P. Matheu<sup>#1,5</sup>, Shivashankar Othy<sup>#1</sup>, Milton L. Greenberg<sup>1</sup>, Tobias X. Dong<sup>1</sup>, Martijn Schuijs<sup>2</sup>, Kim Deswarte<sup>2</sup>, Hamida Hammad<sup>2</sup>, Bart N. Lambrecht<sup>2</sup>, Ian Parker<sup>1,3</sup>, and Michael D. Cahalan<sup>1,4,\*</sup>

<sup>1</sup>Department of Physiology and Biophysics, University of California, Irvine, California, USA.

<sup>2</sup>VIB Inflammation Research Center, University of Ghent, Belgium.

<sup>3</sup>Department of Neurobiology & Behavior, University of California, Irvine, California, USA.

<sup>4</sup>Institute for Immunology, University of California, Irvine, California, USA.

# These authors contributed equally to this work.

### Abstract

Foxp3<sup>+</sup> regulatory T cells (Tregs) maintain immune homeostasis through mechanisms that remain incompletely defined. Here, by two-photon imaging, we examine the cellular dynamics of endogenous Tregs. Tregs are identified as two non-overlapping populations in the T-zone and follicular regions of the lymph node. In the T-zone, Tregs migrate more rapidly than conventional T cells (Tconv), extend longer processes, and interact with resident dendritic cells (DC) and Tconv. Tregs intercept immigrant DCs and interact with antigen-induced DC:Tconv clusters, while continuing to form contacts with activated Tconv. During antigen-specific responses, blocking CTLA4-B7 interactions reduces Treg-Tconv interaction times, increases the volume of DC:Tconv clusters, and enhances subsequent Tconv proliferation *in vivo*. Our results demonstrate a role for altered cellular choreography of Tregs through CTLA4-based interactions to limit T cell priming.

### Keywords

Immunoimaging; two-photon microscopy; immunoregulation; Foxp3; CTLA4; regulatory T cell

---

Regulatory T cells (Tregs) expressing the Foxp3 transcription factor constitute a critical component of peripheral immune homeostasis and tolerance. Several autoimmune and inflammatory pathologies in humans are associated with functional defects in Tregs, and

---

Users may view, print, copy, and download text and data-mine the content in such documents, for the purposes of academic research, subject always to the full Conditions of use:[http://www.nature.com/authors/editorial\\_policies/license.html#terms](http://www.nature.com/authors/editorial_policies/license.html#terms)

\*Corresponding Author: Michael D. Cahalan (mcahalan@uci.edu).

<sup>5</sup>Present address: University of California San Francisco Diabetes Center, UCSF, California, USA.

### AUTHOR CONTRIBUTIONS

M.P.M., S.O., M.G., and M.D.C. designed experiments; M.P.M., S.O., M.L.G., T.X.D., M.S., and K.D. performed experiments; M.P.M., S.O., and M.G. analyzed imaging and flow cytometry data; M.P.M., M.D.C., I.P., S.O., H.H., and B.N.L. wrote the manuscript.

Competing financial interests: The authors declare no competing financial interests.

depletion of Tregs in experimental animals leads to systemic autoimmune and allergic disease accompanied by unchecked lymphoproliferation<sup>1-4</sup>. Expression of an inhibitory member of the immunoglobulin super-family, cytotoxic T lymphocyte antigen 4 (CTLA4) by Tregs is critical for their function. The loss of Treg-specific CTLA4 expression or treatment with a blocking antibody lead to potentially lethal T-cell mediated autoimmune pathology<sup>5-8</sup>. Moreover, polymorphisms in human CTLA4 are linked to the development of autoimmune diseases, including type I diabetes and primary progressive multiple sclerosis<sup>9</sup>. Although it is now established that Tregs and their expression of CTLA4 are both indispensable for the maintenance of immune homeostasis<sup>4-6,10</sup>, the underlying cellular and molecular mechanisms of CTLA4-mediated suppression are not well understood<sup>11</sup>. In vitro studies of APC-free T cell cultures have demonstrated that Tregs directly suppress both CD4<sup>+</sup> and CD8<sup>+</sup> T cell proliferation in a contact-dependent, antigen-independent manner<sup>12,13</sup>. However, *in vivo* data are lacking on how endogenous Tregs interact with antigen-presenting cells (APC) and conventional T cells (Tconvs).

Two-photon (2P) microscopy allows detailed observation and analysis of the spatio-temporal choreography of live cell-cell interactions within the native tissue environment of the lymph node, secondary lymphoid organs and peripheral tissues<sup>14,15</sup>. In the lymph node, naive CD4<sup>+</sup> T cells exhibit three distinct phases of behavior in relation to dendritic cells (DCs) during initiation of an immune response<sup>16</sup>: 1) dynamic scanning with transient interactions with antigen-bearing DCs; 2) formation of dynamic clusters in which multiple T cells stop migrating freely and form stable contacts with DCs; and 3) disengagement of T cells from DCs, followed by swarming behavior and subsequent antigen-specific T cell proliferation. Previous 2P imaging studies have investigated Treg-induced suppression during T cell priming either by addition of *in vitro*-separated CD4<sup>+</sup> CD25<sup>+</sup> T cells<sup>17-21</sup> or by diphtheria toxin-induced depletion of Tregs<sup>22</sup>. Notably, no previous studies have imaged endogenous Tregs in the context of both Tconvs and DCs. Simultaneous and direct imaging of endogenous Tregs together with naïve T cells and dendritic cells would permit insight into the cellular behavior and *in vivo* mechanisms that underlie immunoregulation.

Here, using 2P microscopy of lymph nodes from Foxp3<sup>EGFP</sup> mice, we have characterized the dynamics of unperturbed, endogenous Tregs interacting with Tconv and with DCs under steady-state conditions; in the presence of LPS-activated DCs as a model for inflammation; and during antigen-specific CD4 T cell priming. We further demonstrate the crucial involvement of CTLA4-B7 interactions in determining cellular dynamics among Tregs, conventional T cells, and DCs *in vivo*.

## RESULTS

### Imaging regional differences in Treg dynamics

To visualize endogenous Treg cells, we screened mouse strains that express fluorescent proteins specific to Tregs, and identified Foxp3<sup>EGFP</sup> mice as optimal for 2P imaging. Developed by Haribhai *et al.*, Foxp3<sup>EGFP</sup> mice contain a bicistronic Foxp3-EGFP gene that induces reliable co-expression of EGFP and Foxp3 in *bona fide* endogenous Tregs<sup>23</sup>. EGFP<sup>+</sup> Tregs were clearly visualized by 2-photon imaging of explanted lymph nodes without exogenous labeling or adoptive transfer (**Fig. 1a**). Mapping the distribution of Tregs with

respect to CFP<sup>+</sup> CD19<sup>+</sup> B cells and CMTMR-labeled CD4<sup>+</sup> CD25<sup>-</sup> T (Tconv) cells revealed that Tregs are abundant in the T cell zone, and are also present at lower density within B cell follicles and in the sub-capsular space (**Fig. 1b**, **Supplementary Video 1**). Time-lapse images of Tregs and associated tracks indicated little or no active exchange between follicle and adjacent T-zone (**Fig. 1c** and **Supplementary Video 2**). Their basal motility characteristics, morphology, and choreography clearly differed between locations within the lymph node. Mean velocities of Tregs in the T cell zone ( $14.6 \pm 0.2 \mu\text{m}/\text{min}$ ) were significantly higher than follicular Tregs ( $12.9 \pm 0.1 \mu\text{m}/\text{min}$ ,  $p < 0.001$ ). Near or at the capsule, Tregs migrated more slowly ( $9.5 \pm 0.2 \mu\text{m}/\text{min}$ ; **Fig. 1d**), many along collagen fibers (**Supplementary Fig. 1a** and **Supplementary Video 3**). The collagen-interacting Tregs migrated more slowly than other Tregs within 50  $\mu\text{m}$  of the capsule (**Supplementary Fig. 1b**). Deeper in the paracortex (>50  $\mu\text{m}$  below the capsule), Tregs moved rapidly and extended cellular processes (**Fig. 1e** and **Supplementary Video 4**). Within the T-cell zone, Tregs exhibited higher mean velocities ( $13.9 \pm 0.17 \mu\text{m}/\text{min}$ ) than colocalized Tconv cells ( $12.0 \pm 0.2 \mu\text{m}/\text{min}$ ,  $p < 0.001$ ; **Fig. 1f**). Moreover, Tregs extended longer cellular processes than colocalized Tconvs (**Supplementary Fig. 1c**); and follicular Tregs were, on average, even more elongated (**Supplementary Fig. 1d**). Close examination under steady-state conditions in the absence of antigen revealed cell-cell contacts between Treg and Tconv cells (**Fig. 1g**).

In summary, under steady-state conditions two non-overlapping populations of Tregs explore the T-zone and the follicle. Follicular Tregs (fTregs) have been identified previously as CD4<sup>+</sup> Foxp3<sup>+</sup> cells expressing CXCR5 and Bcl6<sup>24,25</sup>. Endogenous Tregs in the T cell zone are the most rapidly motile cells in the lymph node reported to date. In the remainder of this report, we focus on the dynamics of Tregs interacting with Tconvs and DCs in the Tzone.

### Tregs engage resident DCs and Tconv cells

To image endogenous Tregs, resident DCs, and Tconvs simultaneously, we crossed Foxp3-EGFP male mice with CD11c-EYFP reporter female mice<sup>26</sup>. In the resultant F1 heterozygote females, 50% of Foxp3<sup>+</sup> Tregs express EGFP<sup>23</sup>, and EYFP is highly expressed in the lymph node-resident DCs. CMTMR-labeled Tconv cells were then adoptively transferred into these F1 mice, followed by lymph node imaging 24 hr after cells were allowed to equilibrate (**Fig. 2a**). The highly dynamic endogenous Tregs (**Fig. 2b,c** and **Supplementary Video 5**) interacted with CD11c-EYFP<sup>+</sup> resident DCs, forming transient contacts that lasted longer ( $3.3 \pm 0.4 \text{ min}$ ) than interactions between Tconvs and DCs ( $2.5 \pm 0.3 \text{ min}$ ,  $p < 0.004$ , **Fig. 2d**). In the female heterozygous recipient population, only half of the Tregs are GFP<sup>+</sup>; therefore, the actual mean frequency of Treg:DC contacts would be twice that observed (**Fig. 2e**). Thus, a single DC makes contact with  $8.6 \pm 1.1$  Tregs/hr. Given the mean frequency of contacts between endogenous Tregs and resident DCs and their average contact duration of 3.3 min, our measurements indicate that a lymph node-resident DC is in contact with at least one Treg for 28.4 min/hr – *i.e.*, nearly half of the time. Conventional CD4 T cells briefly interacted with Tregs under basal conditions, encountering up to 13.4 Tregs/hour (**Fig. 2e**) for an average of 1:36 min:sec. Therefore, a single Tconv cell spends an average of 21.5 min/hr (36% of the time) in contact with endogenous Tregs.

These results demonstrate that individual Tregs, although less abundant than Tconv cells, are highly active and frequently encounter both DCs and Tconv under basal conditions.

### Activated migratory DCs are intercepted by Tregs

Resident DCs in the LN constitutively present low levels of self-antigens, and the TCR repertoire of Tregs is skewed toward self-antigen recognition<sup>27,28</sup>. Accordingly, we sought to define the interactions between Tregs and activated, migratory DCs from the periphery. Subcutaneous injection of CMTMR-labeled LPS-activated bone marrow-derived DCs (LPS-DCs) into a Foxp3-EGFP animal followed by imaging at 24 hr revealed the highest density of DCs on and around collagen fibers just under the lymph node capsule (**Fig. 3a**). In this region of the lymph node, Tregs readily interacted with and surrounded immigrant DCs, while forming both brief and extended LPS-DC:Treg contacts (**Fig. 3b**). Strikingly, some Tregs established long-lived (up to 40 min) contacts with LPS-DCs near the capsule (**Fig. 3c,d** and **Supplementary Video 6**).

To investigate LPS-DCs and Tregs in the presence of antigen-specific T cells, we transferred labeled OTII cells (**Fig. 3e**) and observed that LPS-DCs were surrounded by endogenous Tregs (**Fig. 3f** and **Supplementary Video 7**). Under these conditions, average Treg contact durations with LPS-DCs were significantly longer (**Fig. 3g**;  $5:53 \pm 0:38$ , min:sec), as compared to both Tconv:LPS-DC ( $2:53 \pm 0:22$ , min:sec) and basal Treg:DC interactions ( $3:14 \pm 0:28$ , both  $p < 0.001$ ; cf. **Fig. 3g** and **Fig. 2d**). Consistent with results from WT Tconv cells, endogenous Treg velocities were significantly higher than adoptively transferred OTII Tconv cells; however, endogenous Tregs slowed significantly as they interacted with LPS-DCs while OTII T cell velocities were unaltered (**Fig. 3h**).

These results led us to examine whether the Treg:DC interactions visualized near the lymph node capsule may lead to the activation of endogenous Tregs<sup>29,30</sup>. Indeed, a higher percentage of CD4 T cells were CD69<sup>+</sup>Foxp3<sup>+</sup> in animals injected with LPS-DCs, compared to control animals (**Supplementary Fig. 2**). Contralateral lymph nodes also had an increased number of CD69<sup>+</sup>Foxp3<sup>+</sup> cells. Our results thus demonstrate that endogenous Tregs interact with activated LPS-DCs draining into the lymph node from the periphery. Prolonged interactions take place near the capsule, and reduce Treg velocity significantly. We infer that such prolonged interactions with immigrant LPS-DCs lead to activation of endogenous Tregs.

### Treg interactions with DC and Tconv during priming

To examine Treg behavior during an antigen-specific response, we imaged OTII Tconv cells, Ova-pulsed DCs (Ova-DCs), and Tregs at a critical point in T cell activation, 12 hr after the transfer of antigen-specific OTII Tconv cells (**Fig. 4a**). This timing matches the initial formation of naïve CD4<sup>+</sup> T cell clusters around antigen-bearing DCs (phase II of T cell activation)<sup>16</sup>. As expected, OTII Tconv cells formed clusters around Ova-DCs. We further observed that Tregs form dynamic contacts with both DCs and antigen-specific Tconv cells (**Fig. 4b** and **Supplementary Video 6**). Although Tconv cells slowed as they interacted with Ova-DCs, no significant change in Treg velocity was observed compared to steady-state conditions (**Fig. 4c** cf. **Fig. 1d**). Treg contact histories illustrate that Tregs spent

more time in contact with responding Tconv cells (**Fig. 4d**, red bars), than with Ova-DCs (green bars); and were often in contact with both (blue bars). However, in several instances, Tregs transitioned from interacting with both the DC and responding T cell to maintain an interaction with the responding Tconv cell alone (**Fig. 4e** and **Supplementary Video 8**). Therefore, during T cell priming, Tregs engage dynamic clusters of DCs and Tconv cells making frequent, brief contacts but without significant slowing.

### Blocking CTLA4 enhances clustering and limits Treg contacts

Cytotoxic T lymphocyte antigen 4 (CTLA4) expressed on Tregs is indispensable for maintenance of immune homeostasis, and treatment with a blocking antibody leads to T-cell-mediated autoimmune disease<sup>5-8</sup>. Based on this, we examined the effect of blocking CTLA4 on the dynamics of Tregs during an antigen-specific T cell response. Using the T cell priming protocol of Fig. 4, we injected antigen-primed Foxp3<sup>EGFP</sup> mice with  $\alpha$ CTLA4 or isotype control (ITC) antibody 30 min after transfer of OTII Tconvs and 4 hr before imaging (**Fig. 5a**). OTII Tconv cell dynamics were visibly altered following  $\alpha$ CTLA4 treatment. Stable clusters of OTII T cells formed around Ova-DCs, and Tregs were excluded from these clusters (**Fig. 5b**), thereby reducing Treg interactions with DCs.  $\alpha$ CTLA4 treatment enhanced Tconv cluster stability and prevented Tregs from making extensive DC contact (**Supplementary Video 9**), as indicated by tracks of Tregs and OTII Tconv cells (respectively, green and red, **Fig. 5c**) and contact history maps (**Fig. 5d**). In  $\alpha$ CTLA4-treated animals, the percentage of OTII Tconv cells that remained in contact with an Ova-DC for over 20 min (stable contact) was significantly higher (**Fig. 5e**). Indeed, OTII Tconv cell contacts with DCs were significantly longer on average in the presence of  $\alpha$ CTLA4 ( $p < 0.01$ ), whereas Treg interactions with Ova-DCs were not altered (**Fig. 5f**). Collectively, these results indicate that OTII Tconv cell clustering around Ova-DCs is enhanced by blocking CTLA4.

### CTLA4-B7 interactions contribute to Tregfunction

CTLA-4 is known to negatively regulate T cell responses through interactions with costimulatory B7 molecules, B7.1 (CD80) and B7.2 (CD86) on APCs<sup>31</sup>. In vitro and in vivo studies have shown that Tregs can capture B7 ligands from DCs through a process of trans-endocytosis that requires CTLA4 on Tregs<sup>32</sup>. To determine whether  $\alpha$ CTLA4 treatment alters the expression of co-stimulatory ligands on DCs, we transferred LPSDCs into recipients that were treated with control (ITC) or  $\alpha$ CTLA4 antibodies. By flow cytometric analysis, CD80 and CD86 levels were unaffected by  $\alpha$ CTLA4 treatment (**Supplementary Fig. 3**). Although the expression of CD80 and CD86 has been studied most extensively in APCs, we confirm previous observations<sup>33-35</sup> that Tconv cells also express CD86 and up-regulate CD80 and CD86 in vivo within 12-24 hr of priming (**Supplementary Fig. 4a-d**). Furthermore, after stimulation with anti-CD3/CD28 beads in vitro, CD80 and CD86 were upregulated in Tconv cells that had divided at least once, and elevated levels were retained through several divisions (**Supplementary Fig. 4e**). CTLA4 expression was also increased on Tconv cells that had undergone at least one division and, as expected for activated T cells, CD69 expression was significantly increased in proliferating cells (**Supplementary Fig. 5**).

Upregulation of the CTLA4 ligands CD80 and CD86 in Tconv cells suggested that suppressive CTLA4-B7 interactions may not be exclusive to Treg:DC partners, but may contribute to Treg:Tconv interactions. Using  $\alpha$ CTLA4 blocking antibody and the same dosing protocol as in **Fig. 5a**, we first confirmed a previous study<sup>36</sup> that OTII Tconv cells from the draining lymph nodes proliferated more in  $\alpha$ CTLA4-treated animals than in isotype controls (**Fig. 6a, b**). To complement our results using  $\alpha$ CTLA antibody we then used a genetic approach to address whether Tregs mediate CD80/86-dependent Tconv interactions and suppression. We compared proliferation and Treg suppression of wild-type and CD80/86-double knockout Tconv cells in an APC-free in vitro system (to exclude the effect of Tregs on DCs) using anti-CD3 and anti-CD28 coated beads. WT and CD80/86 knockout Tconv cells proliferated comparably in response to  $\alpha$ CD3/CD28 beads (**Fig. 6c**). At a 1:1 ratio, WT Tregs inhibited proliferation of WT Tconvs by  $48\% \pm 1.1\%$  (mean  $\pm$  SEM); however, Treg suppression was significantly reduced in CD80/86 knockout Tconv cells to  $38\% \pm 1.7\%$  ( $p=0.001$ , **Fig. 6d**). Thus, the lack of CD80/CD86 makes Tconv cells less susceptible to suppression by Tregs.

### CTLA4 stabilizes Treg interactions with Tconv cells

Collectively, the above results point toward an important functional role of Treg CTLA4 interactions with CD80/86 on Tconvs. To examine the choreography of these interactions, we compared Treg:Tconv interactions under control conditions (ITC) and following  $\alpha$ CTLA4 treatment. In ITC-treated mice, it was clear that Tregs interacted extensively with Tconvs while also simultaneously interacting with DCs during antigen priming (**Fig. 6e**). In contrast, during  $\alpha$ CTLA4 treatment Tregs did not interact with Tconv in DC clusters (**Fig. 6f**). To quantitatively analyze the role of CTLA4 in stabilizing T cell-T cell interactions, we measured contact durations under steady-state, inflammatory, and priming conditions. Steady-state Tconv:Treg cell contacts, although brief, were significantly longer than Tconv:Tconv cell contacts (**Fig. 6g**). Treg interaction times with Tconvs were prolonged in the presence of LPS-DCs, implying that inflammatory conditions may increase Tconv:Treg adhesion (**Fig. 6g**). During antigen activation of OTII Tconv cells, Tconv:Treg interaction times were substantially increased; and notably,  $\alpha$ CTLA4 treatment during priming reduced Tconv:Treg contact durations to steady-state values (**Fig. 6h**). These results indicate that the stronger interactions between Tconv and Tregs during inflammation and priming are CTLA4-dependent.

In light of the high constitutive expression of CTLA4 by Tregs and induced expression of CTLA4 by Tconvs, as well as apparently conflicting evidence as to whether CTLA4 overrides or has no effect on the TCR-induced stop-signal<sup>37,38</sup>, we also analyzed the effects of  $\alpha$ CTLA4 treatment on OTII Tconv and Treg velocities under both steady-state and priming conditions. In the absence of cognate antigen,  $\alpha$ CTLA4 treatment increased Treg velocity modestly without significantly altering Tconv cell velocity (**Fig. 6i**). Under priming conditions, DC-interacting OTII Tconv velocities were reduced by  $\alpha$ CTLA4 treatment, while at the same time Treg velocities were increased, relative to ITC treatment (**Fig. 6j**). These results are consistent with the well-known observation that velocities are reduced by cellular interactions as cells cluster during priming<sup>14,16</sup>.

## DISCUSSION

Previous *in vitro* and *in vivo* studies have described both contact-dependent and chemokine-mediated mechanisms of suppression by Tregs<sup>11,39,40</sup>. In this study, we employed 2P imaging to directly visualize and characterize the behavior of endogenous Tregs and their interactions with DCs and conventional T cells. Two non-overlapping populations of Tregs were observed in lymph node: one in the T cell zone, and one in the follicle. The follicular population was characterized by its position near the periphery of the lymph node, colocalization with B cells, and lack of exchange with Tregs in the T-zone as defined by colocalization with Tconv cells. Follicular Tregs have been previously described as being retained in the B cell follicle by expression of CXCR5<sup>+</sup> and high local concentrations of CXCL13<sup>24</sup>; and have been shown to regulate germinal center formation<sup>25</sup>. Here, we focus on T-zone Tregs that limit Tconv cell priming.

Several imaging studies used *in vitro*-expanded T cells to infer the effects of Tregs on Tconv cells in lymph node, but without a full consensus on mechanisms of immunoregulation<sup>17,18,21</sup>. Tadokoro *et al.*<sup>18</sup> concluded that Tregs inhibit CD4<sup>+</sup> helper T cell interactions with DCs; Angiari *et al.*<sup>21</sup> found that Treg inhibition of T cell:DC contacts and cluster formation was restricted to the late phases of activation; whereas Mempel *et al.*<sup>17</sup> observed that the addition of Tregs did not affect the long duration interactions between CD8<sup>+</sup> cytotoxic T lymphocytes and antigen-presenting B cell targets. Tang *et al.*<sup>19</sup> imaged adoptively transferred antigen-specific CD4<sup>+</sup>CD25<sup>+</sup> Tregs during immune response to islet antigen and concluded that DC-Treg interactions limit helper T cell activation. Recently, Pace *et al.*<sup>22</sup> indirectly demonstrated that Tregs suppress low-avidity CD8<sup>+</sup> responses to foreign antigens, showing that Treg depletion did not alter the long lasting APC-T cell interactions induced by high-affinity antigen, whereas short duration interactions induced by low affinity antigen were prolonged. While reporting the role of *Mst1* kinase in Tregs, Tomiyama *et al.*<sup>20</sup> suggested an alternative mechanism – that antigen-specific Tregs down-regulate co-stimulatory molecules on DCs but are unlikely to inhibit naïve T cell priming by physically competing for DCs. However, in that study<sup>20</sup> 2P imaging was performed on sliced LN instead of intact or *in vivo* LN, raising caveats regarding damage to tissue architecture. Distinct from previous studies, our results provide evidence for direct physical interaction among endogenous Tregs with Tconv and APCs during an ongoing immune regulation in LN and further highlight the role of CTLA4 in coordinating these interactions. **Figure 7** depicts a summary of cellular choreography, surface markers, and cell interactions measured by contact durations under basal conditions, during inflammation, and during T cell priming.

Under basal conditions in the absence of antigen (**Fig. 7a** top left), Tconv cells move rapidly and in a random-walk search for cognate antigen, sampling DCs with brief interactions<sup>41</sup>. In the present study, we show that Tregs in the T cell zone migrate even faster than Tconv cells and engage both resident DCs and Tconv cells in frequent, brief contacts. Tregs have elongated processes, and contacts with Tconv are characterized by close apposition of membranes. Although Tregs constitute only 5-10% of the total number of T cells in the lymph node, our data indicate that individual Tconvs and resident DCs interact directly with

Tregs with high frequency, and are in contact with at least one Treg 36% and 47% of the time, respectively, under basal conditions.

During inflammation (**Fig. 7a** top right), activated DCs from the periphery enter the lymph node via afferent lymphatics and encounter Tregs near the lymph node capsule. Activated DCs not pulsed with exogenous antigen up-regulate CD80 and CD86, and present self-antigens in the context of MHCII<sup>29,42</sup>. We demonstrate that activated LPS-DCs form prolonged contacts with Tregs and that the presence of LPSDCs causes a significant increase in the proportion of Tregs that are activated. The interactions of Tregs with LPS-activated DCs are reminiscent of prolonged CD4 T cell interactions with dermally-derived antigen-presenting DCs during priming<sup>16</sup>.

When antigen is present on migratory DCs (**Fig. 7a** bottom), the cellular dynamics undergo marked changes that can be divided into three phases as previously described<sup>16</sup>. We show the dynamic behavior and physical interaction of Tregs with Tconvs and DCs during phase II (sustained contact). During this phase, regulatory T cells frequently interact with clusters of APC:Tconv but remain highly motile, suggesting that Tregs transiently scan these clusters. Our results complement a recent study reporting interaction behavior of antigen-specific Tregs with CTLs and APCs in a tumor model<sup>43</sup>. That study and our results suggest that APCs displaying peptide-MHC complexes and co-stimulatory molecules provide a platform for Tconv and Treg interaction. Mechanistically, Tregs have been proposed to regulate immune responses by decreasing CD80 and CD86 on APCs in a CTLA-4 dependent manner, thus rendering APCs less potent for further activation of Tconv cells<sup>32,44-46</sup>. However, in our experiments, in vivo treatment with  $\alpha$ CTLA4 did not alter expression of the costimulatory ligands, CD80 and CD86 in adoptively transferred and LN-recovered DCs. Several in vitro APC-free assays have shown that Tregs are capable of direct inhibition of Tconv cell activation in a contact-dependent and antigen-independent manner<sup>12,47</sup>. We confirm this, and now provide direct evidence for CTLA4-dependent physical interactions between Treg:Tconv cells during immune activation in vivo. Coinciding with phase II of antigen-specific Tconv priming, when cognate Tconv cells interact stably with DCs and high-density Tconv:DC clusters form (8-16 hr), we show that Tconv cells increase their expression of CD80 and CD86 upon activation (**Fig. 7b**), becoming potential targets for CTLA4-mediated interaction with Tregs. In the presence of blocking  $\alpha$ CTLA4 antibody, Tregs appeared oblivious to both DCs and Tconvs, resulting in larger and more stable Tconv:DC clusters and contributing to enhanced T cell proliferation in vivo.

Contact-dependent suppression mediated by B7 molecules on activated T cells was previously proposed by Cantor and colleagues<sup>39</sup>. CD86 is expressed by naïve CD4<sup>+</sup> T cells, and we demonstrate that both CD80 and CD86 are expressed by activated CD4<sup>+</sup> T cells. Using an in vitro, APC-free, genetic approach we show that lack of CD80 and CD86 expression on Tconvs renders them less susceptible to suppression by Tregs. Notably, Treg suppression is not completely abrogated, because multiple mechanisms for Treg suppression of Tconv cell priming may operate simultaneously<sup>11,48,49</sup>. Here, we show that CTLA4 on Tregs limits Tconv clustering around antigen-bearing DCs. We demonstrate that Tregs physically engage Tconv cells that have up-regulated CD80 and CD86. Indeed, we found



that  $\alpha$ CTLA4 treatment disrupts both Treg-Tconv and Treg-DC cell interactions at this early time point of T cell activation (**Fig. 7c**). Moreover, T cell-T cell synapses have been reported to play a critical role in CD8 T cell differentiation through active exchange of cytokines during transient T-T synapse formation<sup>50</sup>. In line with a recent report on the role of CTLA-4 in stabilizing Treg synapses in vitro<sup>51</sup>, our study delineates an important functional role of Tregs to limit priming through CTLA4 interactions with upregulated B7 ligands on Tconv cells in vivo.

Finally, it has been suggested that CTLA4 may play a role in the inhibition of TCR-induced T cell stopping<sup>37,52</sup>, but this is controversial<sup>38</sup>. In our hands, treatment with  $\alpha$ CTLA4 increased steady-state Treg motility while having no effect on Tconv motility. During antigen-specific immune activation, treatment with  $\alpha$ CTLA4 again enhanced Treg motility, but antigen-specific Tconv exhibited a significant decrease in velocity while forming stable clusters with DCs. Considering the role of CTLA4 in stabilizing Treg immune-synapses<sup>51</sup>, enhanced Tconv cell clustering adjacent to DCs could be due to local exclusion of Tregs when CTLA4 is blocked.

## METHODS

### Mice, cell-labeling and reagents

Mice were housed in a clean, pathogen-free facility. Animal care and protocols were reviewed and approved by Institutional Animal Care and Use Committee of the University of California, Irvine and the animal ethics committee of Ghent University (ethical committee number 2013-015), in accordance with European guidelines (directive 2010/63/EU; Belgian Royal Decree of 6 April 2010). Male mice from the C57Bl/6 background were used at 8-12 weeks of age in donor/recipient experiments. Foxp3<sup>EGFP</sup> mice expressing enhanced GFP along with Foxp3 were obtained from Jackson Laboratories (Stock Number 006772). The CD11c-EYFP mouse strain expressing enhanced YFP on the CD11c promoter<sup>26</sup> was a kind gift of M. Nussenzweig (The Rockefeller University, New York, NY). Foxp3<sup>EGFP</sup> male mice were crossed with CD11c<sup>EYFP</sup> female mice to generate F1 heterozygote females. Other mouse strains included  $\beta$ -actin-CFP (Stock Number 004218), T-cell receptor transgenic ova-IA<sup>b</sup>-specific OTII mice (Stock Number 004194), CD80<sup>-/-</sup> CD86<sup>-/-</sup> mice (Stock Number 003610) and wild type C57Bl/6 mice (Stock Number 000664) were purchased from Jackson Laboratories. Cell labeling was performed by suspending 4-6 million cells in 4 ml of RPMI-1640 at 37° C, quenching and washing twice with RPMI-1640 containing 10% FBS (Gibco). Tconv cells were labeled with 10  $\mu$ M CMTMR for 30 min; for proliferation assays, OTII Tconv cells were labeled with 1.6  $\mu$ M CFSE for 7 min; in some analyzed videos (not shown) DCs were labeled blue with 40  $\mu$ M CMF<sub>2</sub>HC for 40 min (Molecular Probes, CellTrace™ series). The following antibodies were purchased from BioLegend and were used at 0.2  $\mu$ g/ml for flow cytometry and 100  $\mu$ g per animal for in vivo blocking: anti-mouse CTLA4 (clone 9H10, Syrian hamster IgG), ITC (hamster IgG), anti-mouse CD4 (clone GK1.5), APC-conjugated anti-mouse V $\alpha$ 2 (clone B20.1), anti-mouse CD69, anti-mouse CD62L, anti-mouse CD80 (clone 16-10A1), and anti-mouse CD86 (clone GL1). All adoptive transfers were performed under anesthesia and mild restraint, via tail-vein injection (T cells) or by subcutaneous injection (DCs) near a draining lymph node.

## Dendritic cell culture and Tconv proliferation assays

Bone marrow-derived dendritic cells (BMDCs) for 2P imaging were generated as described<sup>53</sup>. Briefly, marrow was extracted from the femur of 6-10 weeks old mice and cultured in non-tissue culture treated polystyrene dishes for 9-10 days (Corning™) using RPMI 1640 (Lonza™) supplemented with 1% L-glutamine, 10% fetal calf serum (FCS; Hyclone Inc.), 100 units/ml penicillin, 100 µg/ml streptomycin, 2-βME and GM-CSF, IL-4 and TNFα, as previously described<sup>53</sup>. For *in vivo* proliferation assays IL-4 and TNFα were excluded to enhance antigen uptake during Ova-pulsing. For activated DCs and antigen-specific T-DC interaction imaging studies, DCs were treated with LPS (100 ng/ml) alone or with LPS + Ova (100 µg/ml) for 12-24 hr prior to harvest and injection. CD4<sup>+</sup>CD25<sup>-</sup> T cells (Tconv) were isolated from spleen and lymph nodes of 6-10 week old mice using negative selection (Miltenyi Biotec and StemCell Technologies). For APC-free *in vitro* proliferation, CFSE-labeled WT Tconv cells were co-cultured with anti-CD3/CD28 coated dynabeads (Life Technologies®) at 1:1 ratio according to the manufacturer's protocol. Tregs were added to Tconv at 1:1 ratio for suppression assays. CFSE dilution in live cells (Fixable Viability Dye eFluor® 780 negative gating; eBioscience) was analyzed using BD LSRII flow cytometer. For measuring the effects of αCTLA4 on *in vivo* proliferation, 2 × 10<sup>6</sup> Ova-pulsed DCs were injected s.c. into the footpad of WT mice; after 18 hr, 3 × 10<sup>6</sup> CFSE-labeled OTII Tconv cells were injected intravenously; popliteal lymph nodes were collected on day 3 of Tconv cell transfer; LN from the contralateral hind limb served as immunization control. CFSE dilution in single cells was analyzed by gating on Vα2<sup>+</sup> CFSE<sup>+</sup> population. Activation Indices (AI) were calculated using Equation 1, as described<sup>54</sup>, where M values correspond to the number of cell divisions assessed by CFSE dilution.

$$AI = \frac{M_9 + \frac{127}{128}M_8 + \frac{63}{64}M_7 + \frac{31}{32}M_6 + \frac{15}{16}M_5 + \frac{7}{8}M_4 + \frac{3}{4}M_3 + \frac{1}{2}M_2}{\frac{1}{128}M_8 + \frac{1}{64}M_7 + \frac{1}{32}M_6 + \frac{1}{16}M_5 + \frac{1}{8}M_4 + \frac{1}{4}M_3 + \frac{1}{2}M_2 + M_1} \quad \text{Equation 1}$$

## 2-Photon Imaging

All images were acquired with excitation wavelengths between 890 and 910 nm. Two imaging systems were used. The primary system used is a custom-built 2-photon system based on an Olympus BX5 upright microscope, with excitation generated by a tunable Chameleon femtosecond laser (Coherent). 495 nm and 560 nm dichroic filters were arranged in series to separate blue, green and red signals, and images were collected as previously described<sup>55</sup> at UC Irvine. EGFP and EYFP signals are separated using a 520 nm dichroic filter. Additional data were collected on a Zeiss inverted 710 2-photon system in the Inflammation Research Center (IRC), VIB-U Gent with a Zeiss SP 485 nm, LP 490 nm, LP 555 nm, BP 565-610 nm filter combination arranged in series with blue, green and red PMTs. Both microscopes were fitted with either a 20x (NA = 0.95), 25x (NA = 1.05), or 60x (NA = 1.1) water-immersion objectives, and equipped with 3 PMTs, peristaltic heated perfusion systems (Warner Instruments), thermocouple-based temperature sensors placed next to the tissue. All imaging was carried out on lymph nodes maintained at 37° ± 0.5°C and superfused with RPMI-1640 and medical grade carbogen gas (95% O<sub>2</sub> and 5% CO<sub>2</sub>). Size and velocity comparisons of endogenous Foxp3-eGFP T cells from each microscope were analyzed separately and found to be nearly identical with no significant variation.

## Data Analysis

All image analysis was performed using Imaris software (Bitplane) version 6.5-7.2. Cells were tracked manually and contact durations were measured with 3D rotation to verify contacts. Stable contact formation was defined as any OTII T cell that remained in contact with one DC for a minimum of 20 min. Displayed images in the all figures are maximal intensity projections through the z-axis ('top view'; 50-70  $\mu\text{m}$  depth in this panel) of x-y-z stacks. Flow-cytometry was performed on either a BD LSRII (UC-Irvine and VIB-UGent) or BD LSR-Fortessa (VIB-UGent) and analyzed using FlowJo. Figures were generated using Graphpad Prism and OriginPro8. Statistical analysis was performed using Mann Whitney test (unpaired sample, nonparametric); p values are marked in figures: \*  $p < 0.05$ ; \*\*  $p < 0.01$ ; \*\*\*  $p < 0.001$ ; and \*\*\*\*  $p < 0.0001$ .

## Supplementary Material

Refer to Web version on PubMed Central for supplementary material.

## ACKNOWLEDGMENTS

The authors thank Dr. Lurette Forrest and Dr. Olga Safrina of UC Irvine and Dr. Katrien Moerloose of IRC VIB-UGent for excellent animal care and vivarium support; Rik Verschuere and Charly van Kuijck of IRC VIB-UGent for equipment and machine shop support. This research was supported by NIH grants GM-41514 (M.D.C.), GM-48071 (I.P.), and by postdoctoral fellowships from the George E. Hewitt Foundation for Medical Research (M.P.M. and S.O.) and the European Respiratory Society (M.P.M.).

## Abbreviations

<b><math>\alpha</math>CTLA4</b>	anti-CTLA4 blocking antibody
<b>DC</b>	dendritic cell
<b>ITC</b>	isotype control
<b>LPS</b>	lipopolysachharide
<b>Ova</b>	ovalbumin
<b>Tconv</b>	conventional $\text{CD4}^+\text{CD25}^-$ T cell
<b>Treg</b>	regulatory T cell
<b>2P</b>	two-photon
<b>WT</b>	wild type

## REFERENCES

1. Sakaguchi S, Yamaguchi T, Nomura T, Ono M. Regulatory T cells and immune tolerance. *Cell*. 2008; 133:775–787. [PubMed: 18510923]
2. van der Vliet HJ, Nieuwenhuis EE. IPEX as a result of mutations in FOXP3. *Clin Dev Immunol*. 2007; 2007:89017. [PubMed: 18317533]
3. Wildin RS, Freitas A. IPEX and FOXP3: clinical and research perspectives. *J Autoimmun*. 2005; 25(Suppl):56–62. [PubMed: 16243487]
4. Huter EN, et al. TGF-beta-induced Foxp3+ regulatory T cells rescue scurfy mice. *Eur J Immunol*. 2008; 38:1814–1821. [PubMed: 18546144]

5. Wing K, et al. CTLA-4 control over Foxp3+ regulatory T cell function. *Science*. 2008; 322:271–275. [PubMed: 18845758]
6. Takahashi T, et al. Immunologic self-tolerance maintained by CD25(+)CD4(+) regulatory T cells constitutively expressing cytotoxic T lymphocyte-associated antigen 4. *J Exp Med*. 2000; 192:303–310. [PubMed: 10899917]
7. Waterhouse P, et al. Lymphoproliferative disorders with early lethality in mice deficient in CtlA-4. *Science*. 1995; 270:985–988. [PubMed: 7481803]
8. Tivol EA, et al. Loss of CTLA-4 leads to massive lymphoproliferation and fatal multiorgan tissue destruction, revealing a critical negative regulatory role of CTLA-4. *Immunity*. 1995; 3:541–547. [PubMed: 7584144]
9. Gough SC, Walker LS, Sansom DM. CTLA4 gene polymorphism and autoimmunity. *Immunol Rev*. 2005; 204:102–115. [PubMed: 15790353]
10. Tang Q, et al. Distinct roles of CTLA-4 and TGF-beta in CD4+CD25+ regulatory T cell function. *Eur J Immunol*. 2004; 34:2996–3005. [PubMed: 15468055]
11. Schmidt A, Oberle N, Krammer PH. Molecular mechanisms of treg-mediated T cell suppression. *Front Immunol*. 2012; 3:51. [PubMed: 22566933]
12. Thornton AM, Shevach EM. Suppressor effector function of CD4+CD25+ immunoregulatory T cells is antigen nonspecific. *J Immunol*. 2000; 164:183–190. [PubMed: 10605010]
13. Piccirillo CA, Shevach EM. Cutting edge: control of CD8+ T cell activation by CD4+CD25+ immunoregulatory cells. *J Immunol*. 2001; 167:1137–1140. [PubMed: 11466326]
14. Miller MJ, Wei SH, Parker I, Cahalan MD. Two-photon imaging of lymphocyte motility and antigen response in intact lymph node. *Science*. 2002; 296:1869–1873. [PubMed: 12016203]
15. Germain RN, Robey EA, Cahalan MD. A decade of imaging cellular motility and interaction dynamics in the immune system. *Science*. 2012; 336:1676–1681. [PubMed: 22745423]
16. Miller MJ, Safrina O, Parker I, Cahalan MD. Imaging the single cell dynamics of CD4+ T cell activation by dendritic cells in lymph nodes. *J Exp Med*. 2004; 200:847–856. [PubMed: 15466619]
17. Mempel TR, et al. Regulatory T cells reversibly suppress cytotoxic T cell function independent of effector differentiation. *Immunity*. 2006; 25:129–141. [PubMed: 16860762]
18. Tadokoro CE, et al. Regulatory T cells inhibit stable contacts between CD4+ T cells and dendritic cells in vivo. *J Exp Med*. 2006; 203:505–511. [PubMed: 16533880]
19. Tang Q, et al. Visualizing regulatory T cell control of autoimmune responses in nonobese diabetic mice. *Nat Immunol*. 2006; 7:83–92. [PubMed: 16311599]
20. Tomiyama T, et al. Antigen-specific suppression and immunological synapse formation by regulatory T cells require the Mst1 kinase. *PLoS one*. 2013; 8:e73874. [PubMed: 24040101]
21. Angiari S, et al. Regulatory T cells suppress the late phase of the immune response in lymph nodes through P-selectin glycoprotein ligand-1. *J Immunol*. 2013; 191:5489–5500. [PubMed: 24174617]
22. Pace L, et al. Regulatory T cells increase the avidity of primary CD8+ T cell responses and promote memory. *Science*. 2012; 338:532–536. [PubMed: 23112334]
23. Haribhai D, et al. Regulatory T cells dynamically control the primary immune response to foreign antigen. *J Immunol*. 2007; 178:2961–2972. [PubMed: 17312141]
24. Chung Y, et al. Follicular regulatory T cells expressing Foxp3 and Bcl-6 suppress germinal center reactions. *Nat Med*. 2011; 17:983–988. [PubMed: 21785430]
25. Linterman MA, et al. Foxp3+ follicular regulatory T cells control the germinal center response. *Nat Med*. 2011; 17:975–982. [PubMed: 21785433]
26. Lindquist RL, et al. Visualizing dendritic cell networks in vivo. *Nat Immunol*. 2004; 5:1243–1250. [PubMed: 15543150]
27. Hsieh CS, Zheng Y, Liang Y, Fontenot JD, Rudensky AY. An intersection between the self-reactive regulatory and nonregulatory T cell receptor repertoires. *Nat Immunol*. 2006; 7:401–410. [PubMed: 16532000]
28. Pacholczyk R, Ignatowicz H, Kraj P, Ignatowicz L. Origin and T cell receptor diversity of Foxp3+CD4+CD25+ T cells. *Immunity*. 2006; 25:249–259. [PubMed: 16879995]

29. Wilson NS, El-Sukkari D, Villadangos JA. Dendritic cells constitutively present self antigens in their immature state in vivo and regulate antigen presentation by controlling the rates of MHC class II synthesis and endocytosis. *Blood*. 2004; 103:2187–2195. [PubMed: 14604956]
30. Idoyaga J, et al. Specialized role of migratory dendritic cells in peripheral tolerance induction. *The Journal of clinical investigation*. 2013; 123:844–854. [PubMed: 23298832]
31. Teft WA, Kirchhof MG, Madrenas J. A molecular perspective of CTLA-4 function. *Annu Rev Immunol*. 2006; 24:65–97. [PubMed: 16551244]
32. Qureshi OS, et al. Trans-endocytosis of CD80 and CD86: a molecular basis for the cell-extrinsic function of CTLA-4. *Science*. 2011; 332:600–603. [PubMed: 21474713]
33. Prabhu Das MR, et al. Reciprocal expression of co-stimulatory molecules, B7-1 and B7-2, on murine T cells following activation. *Eur J Immunol*. 1995; 25:207–211. [PubMed: 7531145]
34. Greenfield EA, et al. B7.2 expressed by T cells does not induce CD28-mediated costimulatory activity but retains CTLA4 binding: implications for induction of antitumor immunity to T cell tumors. *J Immunol*. 1997; 158:2025–2034. [PubMed: 9036945]
35. Azuma M, Yssel H, Phillips JH, Spits H, Lanier LL. Functional expression of B7/BB1 on activated T lymphocytes. *J Exp Med*. 1993; 177:845–850. [PubMed: 7679711]
36. Read S, et al. Blockade of CTLA-4 on CD4+CD25+ regulatory T cells abrogates their function in vivo. *J Immunol*. 2006; 177:4376–4383. [PubMed: 16982872]
37. Schneider H, et al. Reversal of the TCR stop signal by CTLA-4. *Science*. 2006; 313:1972–1975. [PubMed: 16931720]
38. Fife BT, et al. Interactions between PD-1 and PD-L1 promote tolerance by blocking the TCR-induced stop signal. *Nat Immunol*. 2009; 10:1185–1192. [PubMed: 19783989]
39. Paust S, Cantor H. Regulatory T cells and autoimmune disease. *Immunol Rev*. 2005; 204:195–207. [PubMed: 15790360]
40. Sakaguchi S, Wing K, Onishi Y, Prieto-Martin P, Yamaguchi T. Regulatory T cells: how do they suppress immune responses? *Int Immunol*. 2009; 21:1105–1111. [PubMed: 19737784]
41. Miller MJ, Hejazi AS, Wei SH, Cahalan MD, Parker I. T cell repertoire scanning is promoted by dynamic dendritic cell behavior and random T cell motility in the lymph node. *Proc Natl Acad Sci U S A*. 2004; 101:998–1003. [PubMed: 14722354]
42. Scheinecker C, McHugh R, Shevach EM, Germain RN. Constitutive presentation of a natural tissue autoantigen exclusively by dendritic cells in the draining lymph node. *J Exp Med*. 2002; 196:1079–1090. [PubMed: 12391019]
43. Bauer CA, et al. Dynamic Treg interactions with intratumoral APCs promote local CTL dysfunction. *The Journal of clinical investigation*. 2014; 124:2425–2440. [PubMed: 24812664]
44. Onishi Y, Fehervari Z, Yamaguchi T, Sakaguchi S. Foxp3+ natural regulatory T cells preferentially form aggregates on dendritic cells in vitro and actively inhibit their maturation. *Proc Natl Acad Sci U S A*. 2008; 105:10113–10118. [PubMed: 18635688]
45. Oderup C, Cederbom L, Makowska A, Cilio CM, Ivars F. Cytotoxic T lymphocyte antigen-4-dependent down-modulation of costimulatory molecules on dendritic cells in CD4+ CD25+ regulatory T-cell-mediated suppression. *Immunology*. 2006; 118:240–249. [PubMed: 16771859]
46. Thauland TJ, Koguchi Y, Dustin ML, Parker DC. CD28-CD80 Interactions Control Regulatory T Cell Motility and Immunological Synapse Formation. *J Immunol*. 2014
47. Thornton AM, Shevach EM. CD4+CD25+ immunoregulatory T cells suppress polyclonal T cell activation in vitro by inhibiting interleukin 2 production. *J Exp Med*. 1998; 188:287–296. [PubMed: 9670041]
48. Walker LS, Sansom DM. The emerging role of CTLA4 as a cell-extrinsic regulator of T cell responses. *Nat Rev Immunol*. 2011; 11:852–863. [PubMed: 22116087]
49. Wing K, Yamaguchi T, Sakaguchi S. Cell-autonomous and -non-autonomous roles of CTLA-4 in immune regulation. *Trends Immunol*. 2011; 32:428–433. [PubMed: 21723783]
50. Gerard A, et al. Secondary T cell-T cell synaptic interactions drive the differentiation of protective CD8+ T cells. *Nat Immunol*. 2013; 14:356–363. [PubMed: 23475183]

51. Dilek N, et al. Targeting CD28, CTLA-4 and PD-L1 costimulation differentially controls immune synapses and function of human regulatory and conventional T-cells. *PloS one*. 2013; 8:e83139. [PubMed: 24376655]
52. Lu Y, Schneider H, Rudd CE. Murine regulatory T cells differ from conventional T cells in resisting the CTLA-4 reversal of TCR stop-signal. *Blood*. 2012; 120:4560–4570. [PubMed: 23047820]
53. Matheu MP, Sen D, Cahalan MD, Parker I. Generation of bone marrow derived murine dendritic cells for use in 2-photon imaging. *J Vis Exp*. 2008
54. Sen D, Deerinck TJ, Ellisman MH, Parker I, Cahalan MD. Quantum dots for tracking dendritic cells and priming an immune response in vitro and in vivo. *PloS one*. 2008; 3:e3290. [PubMed: 18820727]
55. Matheu MP, et al. Toll-like receptor 4-activated B cells out-compete Toll-like receptor 9-activated B cells to establish peripheral immunological tolerance. *Proc Natl Acad Sci U S A*. 2012; 109:E1258–1266. [PubMed: 22511718]

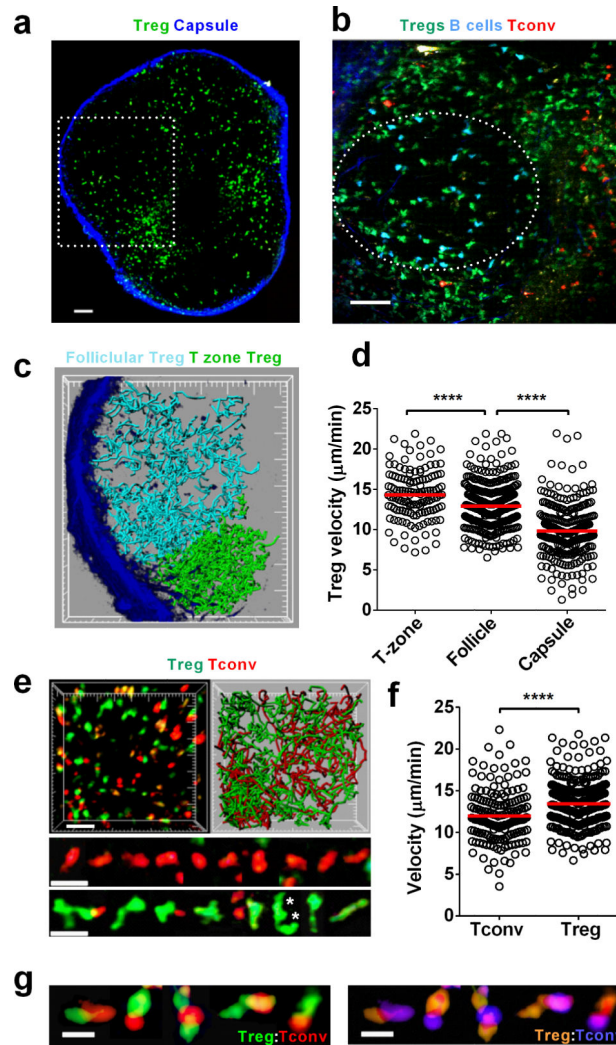


**Figure 1.** Endogenous Foxp3<sup>+</sup> Treg regional behavior and interaction with Tconvs. **(a)** Tregs in inguinal lymph node from a Foxp3<sup>EGFP</sup> mouse under steady-state conditions. Green, EGFP endogenous Tregs; blue, second-harmonic collagen signal in capsular boundary. Single plane image, scale bar = 100 μm. White square represents area imaged in (c). See **Supplementary Video 2.** **(b)** T-zone and follicular Tregs (both green), visualized 72 hr after adoptive transfer of CFP<sup>+</sup>CD19<sup>+</sup> B cells (blue) and CMTMR-labeled Tconv cells (red). Note Tregs colocalized with B cells within the dotted outline, and at higher density with Tconv cells throughout the T cell zone. Scale bar = 50 μm. **(c)** Non-overlapping populations of Tregs in the T-zone and the follicle. Treg movements represented by tracks within (light blue tracks) and outside the B cell follicle (bright green). Cells tracked over 29:38 (min:sec); 35 μm z stack, 50 μm tick marks. **(d)** Treg velocities in three regions of the lymph node. Each circle represents mean velocity in the T cell zone (n = 174 tracks); in the follicle (n = 397 tracks); and within 50 μm of the capsule (n = 343 tracks). Data pooled from 4 experiments. Open circles represent measurements from individual cell tracks; red bars indicate overall mean values; and p values are marked as \* p < 0.05, \*\* p < 0.01, \*\*\* p <

0.001, and \*\*\*\*  $p < 0.0001$  Mann–Whitney U test. **(e)** CMTMR-labeled Tconv cells adoptively transferred 24 hr before imaging and tracked with Tregs over 12 min. Still image (top left, scale bar = 30  $\mu\text{m}$ ) and corresponding tracks (top right) of Tconv cells (red) and Tregs (green) in the T-zone. Lower panels: magnified views of representative individual Tconv cells and endogenous Tregs (scale bars = 20  $\mu\text{m}$ ). Asterisks mark cellular processes. See **Supplementary Video 4**. **(f)** Velocities of individual Tregs ( $n = 217$  tracks) and Tconvs ( $n = 166$  tracks) in the T-zone. Data pooled from 3 experiments. **(g)** Tconvs (red) and Tregs (green) in the absence of antigen; right panel pseudocolored to highlight areas of contact; scale bars = 10  $\mu\text{m}$ .



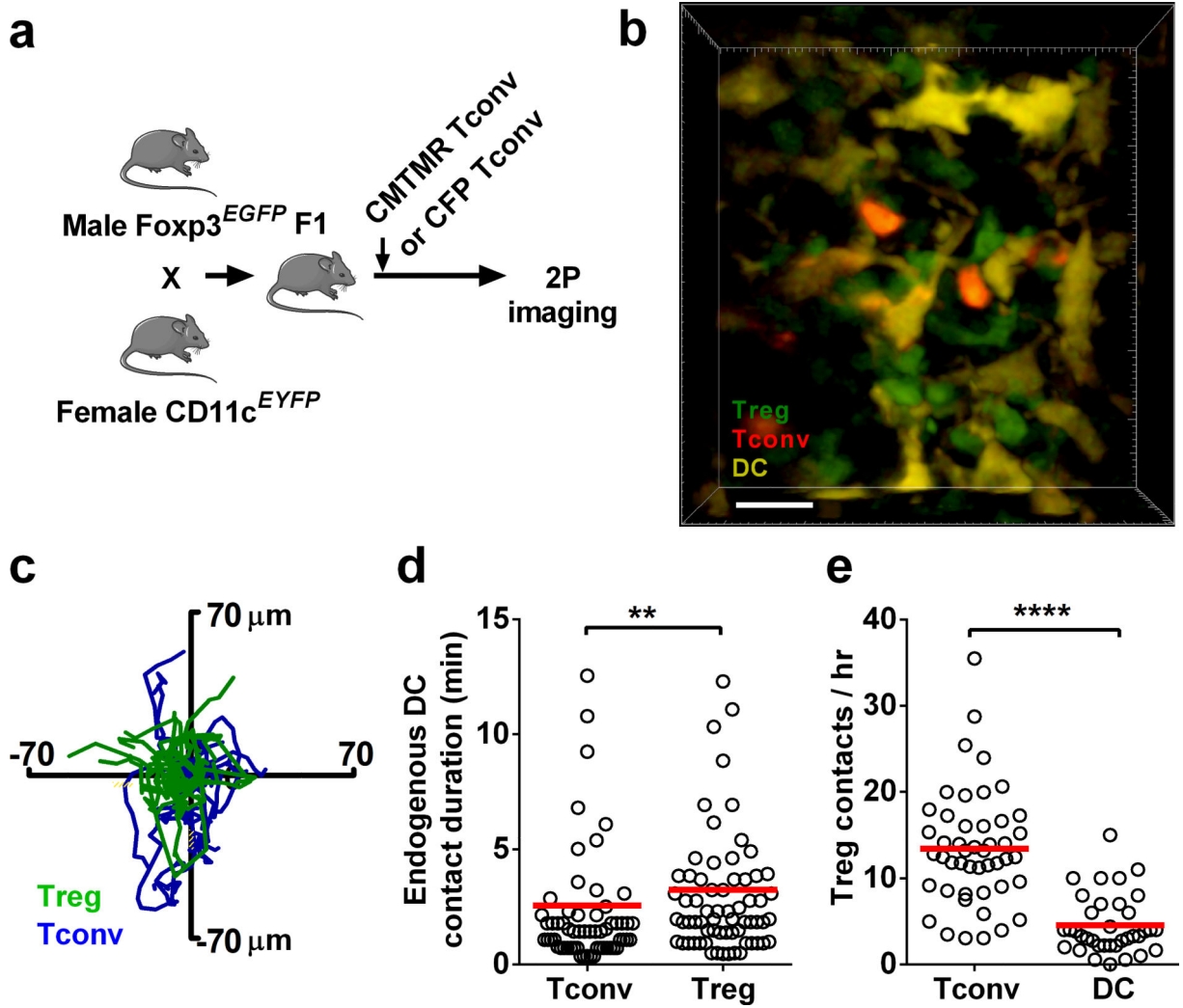


**Figure 2.**

Tregs interact with LN-resident DCs. **(a)** Experimental design to visualize endogenous Tregs together with resident DCs and Tconv cells. CMTMR-labeled Tconv cells from wild type C57Bl/6 mice, or CFP<sup>+</sup> Tconv cells from  $\beta$ -actin-CFP mice were adoptively transferred 12 hr or 4 days, respectively, prior to imaging, into F1 of  $Foxp3^{EGFP}$  x  $CD11c^{EYFP}$  mice.

**(b)** Interactions among Tconv cells (red), resident DCs (yellow), and Tregs (green) under steady-state conditions. Scale bar = 20  $\mu$ m, see **Supplementary Video 5**.

**(c)** Superimposed Treg (green) and Tconv (blue) tracks, z compressed and normalized to DC position at center ( $x, y, = 0, 0$ ). Data from CFP<sup>+</sup> Tconv cells are shown; similar results were obtained with CMTMR-labeled Tconv cells. Cells were tracked over 15:21 (min:sec).

**(d)** Contact durations between cell pairs: Tconvs interacting with DCs ( $n = 61$ ); Tregs interacting with DCs ( $n = 67$ ). Data from CFP<sup>+</sup> Tconv cells are shown, and are also representative of results with CMTMR-labeled Tconv cells. 3 separate experiments, imaging duration >1 hr.

**(e)** Observed contact frequencies with endogenous Tregs by labeled Tconvs ( $n = 47$ ) and by resident DCs ( $n = 36$ ). 2 experiments.

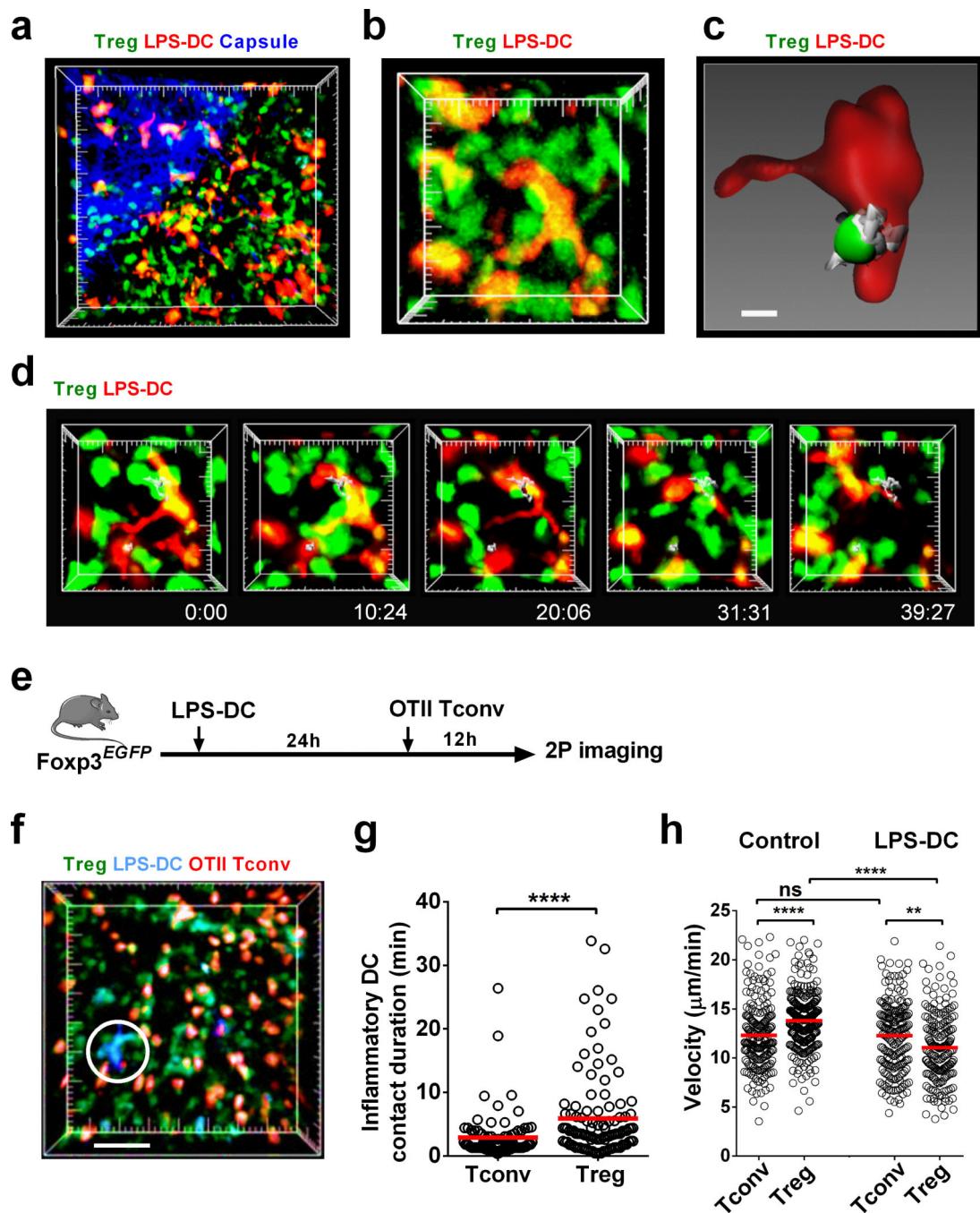


**Figure 3.**

Tregs engage immigrant DCs near the lymph node capsule. **(a)** LPS-activated CMTMR-labeled DCs (red) imaged in the draining inguinal lymph node 24 hr after subcutaneous injection into a Foxp3<sup>EGFP</sup> mouse, showing immigrant DCs encountering and making contact with numerous endogenous Tregs (green) directly beneath the collagen capsule (blue) of the lymph node (major tick marks = 20 µm, 50 µm z-stack). See **Supplementary Video 6**. **(b)** Close-up image of a DC (red) near the collagen capsule and its interactions with several Tregs (green). Major tick marks = 10 µm. **(c)** Space-filled rendering of the DC

(red) from (b) and an associated Treg (green) with track (grey, 39:27 min:sec duration of imaging), showing the close association between Treg and DC (scale bar = 5  $\mu$ m). (d) Time sequence (times shown in min:s) showing interactions of Tregs (green with grey tracks) engaging recently immigrated DCs (red). (e) Experimental design to examine the effect of LPS-activated DCs on OTII Tconv cells and Tregs. LPS-activated DCs from a ECFP mouse were injected into a Foxp3<sup>EGFP</sup> mouse followed by adoptive transfer of CMTMR-labeled OTII Tconv cells at 24 hr and 2P imaging in the draining lymph node 12 hr later. (f) Snapshot showing adoptively transferred OTII Tconv cells (red), LPS activated DC (blue), and Tregs (green). Scale bar = 30  $\mu$ m. See **Supplementary Video 7**. (g) Contact durations of Tregs with LPS-DCs (n = 110 contacts) and Tconvs with LPS-DCs (88 contacts). Data pooled from 3 experiments each. (h) Effect of LPS-activated DCs on Treg velocities. Control velocities in the absence of LPS-DCs: Treg n = 296; OTII Tconv cells n = 213. In the presence of LPS DCs: OTII Tconv cell velocity did not change appreciably (p = 0.7, n = 207, Mann–Whitney U test) whereas Treg velocity was reduced (n = 193) Data pooled from 3 experiments each.

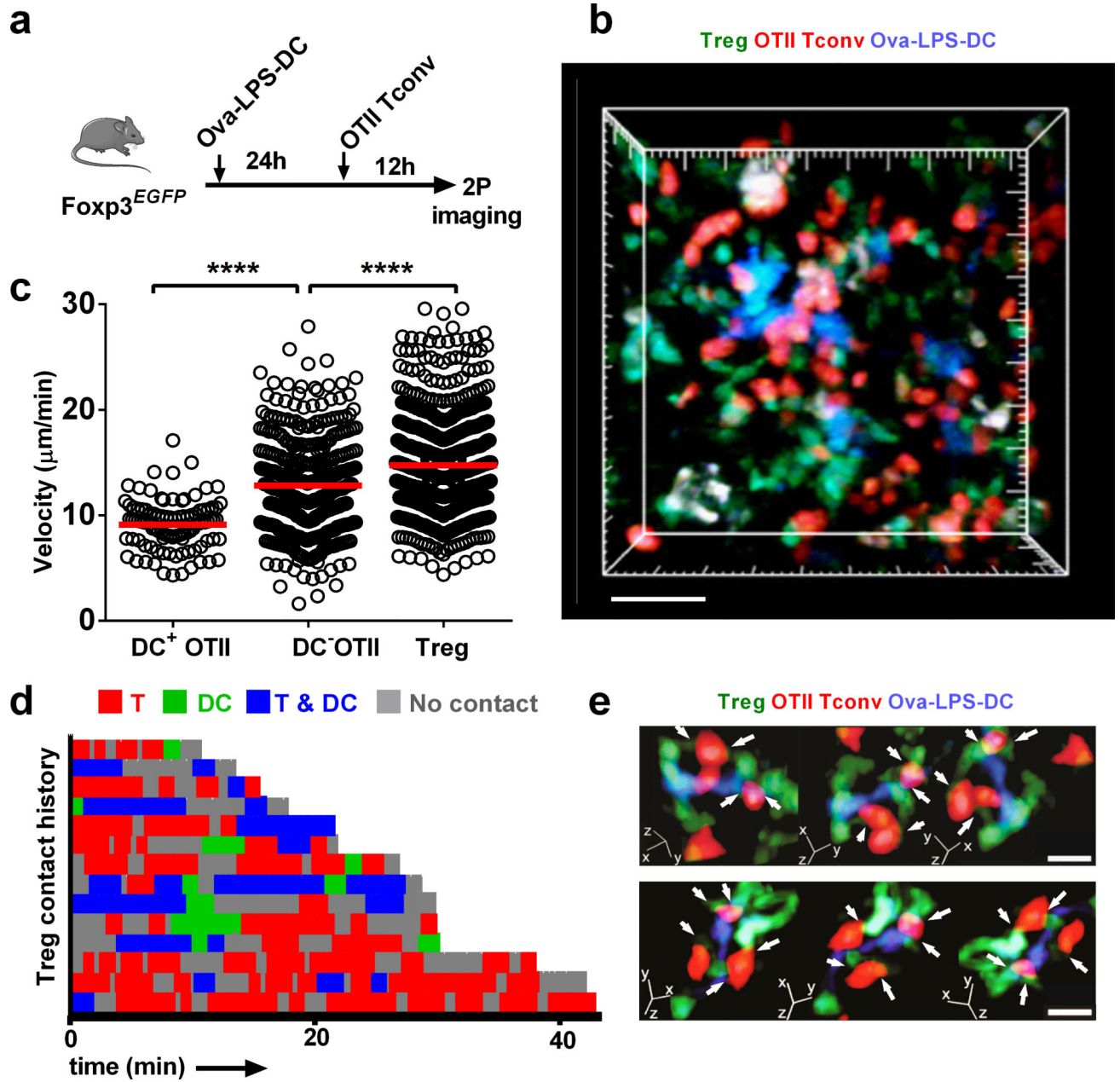


**Figure 4.** Dynamics of Tregs during antigen-specific Tconv priming. **(a)** Experimental design to examine endogenous Treg behavior during an immune response. Ova-pulsed DCs were adoptively transferred into  $Foxp3^{EGFP}$  mice 24 hr prior to transfer of CMTMR-labeled OTII Tconv cells; imaging was performed 12 hr after OTII T cell transfer. **(b)** Tconv-DC clusters. Still image showing DCs (blue), OTII Tconv cells (red), and Tregs (green). Scale bar = 50  $\mu$ m, see **Supplementary Video 8**. **(c)** Tconv and Treg velocities. Mean track velocities of OTII T cells were separated into those that interacted with a DC ( $DC^+$  OTII,  $n = 99$ ) and those that did not ( $DC^-$  OTII,  $n = 426$ ). Treg velocities,  $n = 811$ . Data are pooled from 3 experiments. **(d)** Contact history map for 14 representative Tregs. Each horizontal bar

represents times when a single Treg was alone (grey), in contact with a Tconv (red), in contact with a DC (blue), or in contact with DC:Tconv pairs (green). (e) Close-up images of Treg-Tconv cell contacts (white arrows) in the vicinity of a DC. The panel shows 3-way rotations at two time points, 67 sec apart. Scale bar = 10  $\mu\text{m}$ .

Author Manuscript

Author Manuscript

Author Manuscript

Author Manuscript

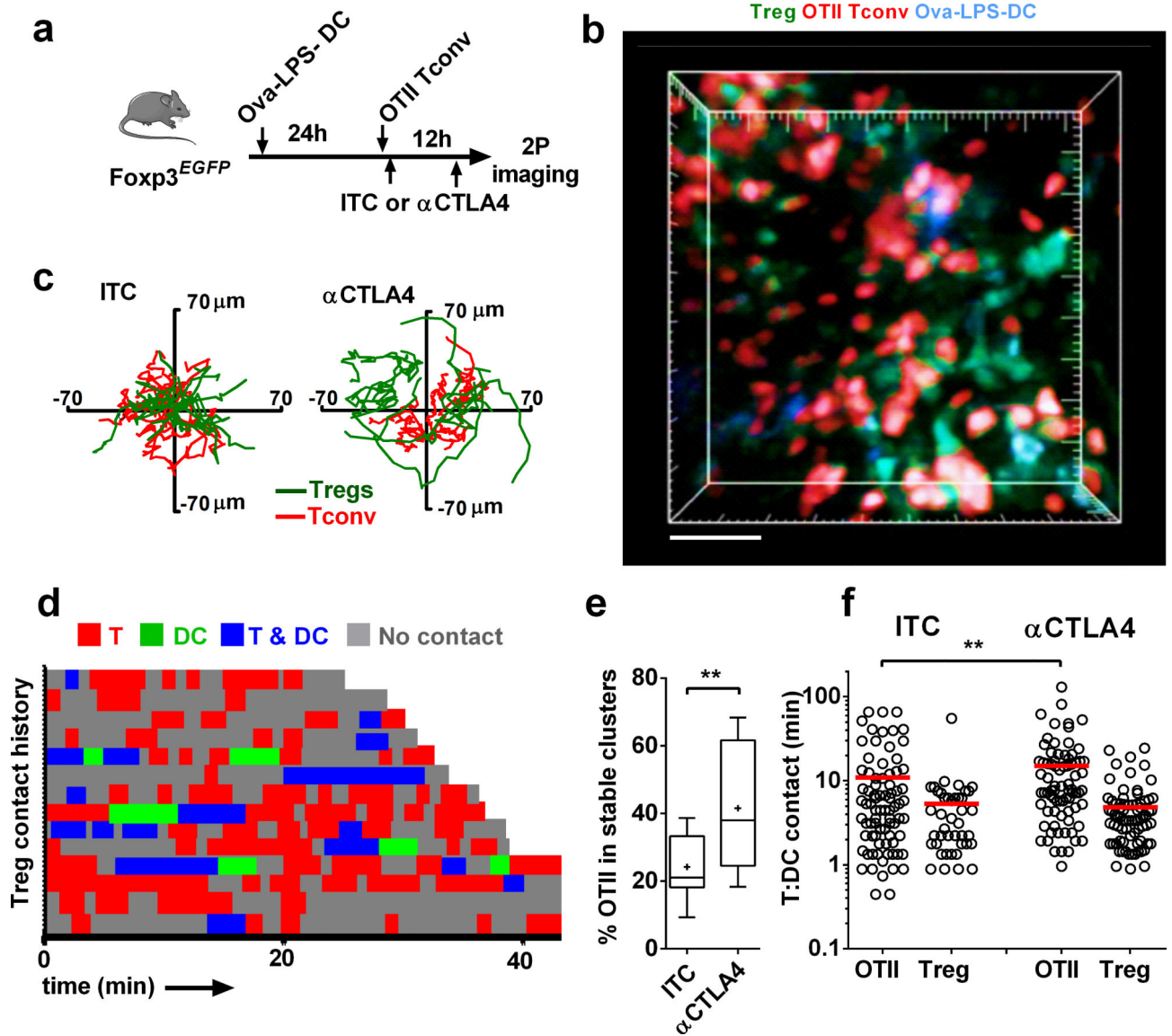


**Figure 5.** Tregs engage antigen-specific clusters of DCs and Tconv cells in a CTLA4-dependent manner. (a) Experimental design to image the role of CTLA4-B7 in Treg interactions. Ova-pulsed DCs from ECFP mice were adoptively transferred into Foxp3<sup>EGFP</sup> mice 24 hr prior to CMTMR-labeled OTII Tconv cells; imaging was performed 12 hr after OTII Tconv cell transfer. Animals received 150 µg of either ITC or αCTLA4, 30 min after adoptive transfer and 4 hr prior to imaging. (b) Still image showing DCs (blue), OTII Tconv cells (red), and Tregs (green) in a node from αCTLA4-treated mouse. Scale bar = 50 µm, see **Supplementary Video 9**. (c) Superimposed tracks of OTII T cells (red) and Tregs (green), with their origins normalized to the center of a DC. Cells were tracked for 10:14 min:sec. n = 21 for ITC and 34 for αCTLA4. (d) Treg contact history map. Each horizontal bar represents a single Treg, with contacts color coded as in Fig. 4d. Note the shorter red and blue bars as compared to Fig. 4d, indicating that Tregs spend less time interacting with

Tconv cells and DCs in the presence of  $\alpha$ CTLA4. **(e)** The percentage of OTII T cells in stable contact with a DC was increased by  $\alpha$ CTLA4 treatment, compared to control (n = 21 and 14, respectively). 20 min imaging period minimum. **(f)** Tconv and Treg contact durations with antigen-bearing DCs. OTII Tconv:DC contact durations are increased in the presence of  $\alpha$ CTLA4 (n = 78) relative to ITC control (n = 80). Treg:DC contact durations were shortened in the presence of  $\alpha$ CTLA4 (n = 42) relative to ITC (n = 83).

Author Manuscript

Author Manuscript

Author Manuscript

Author Manuscript

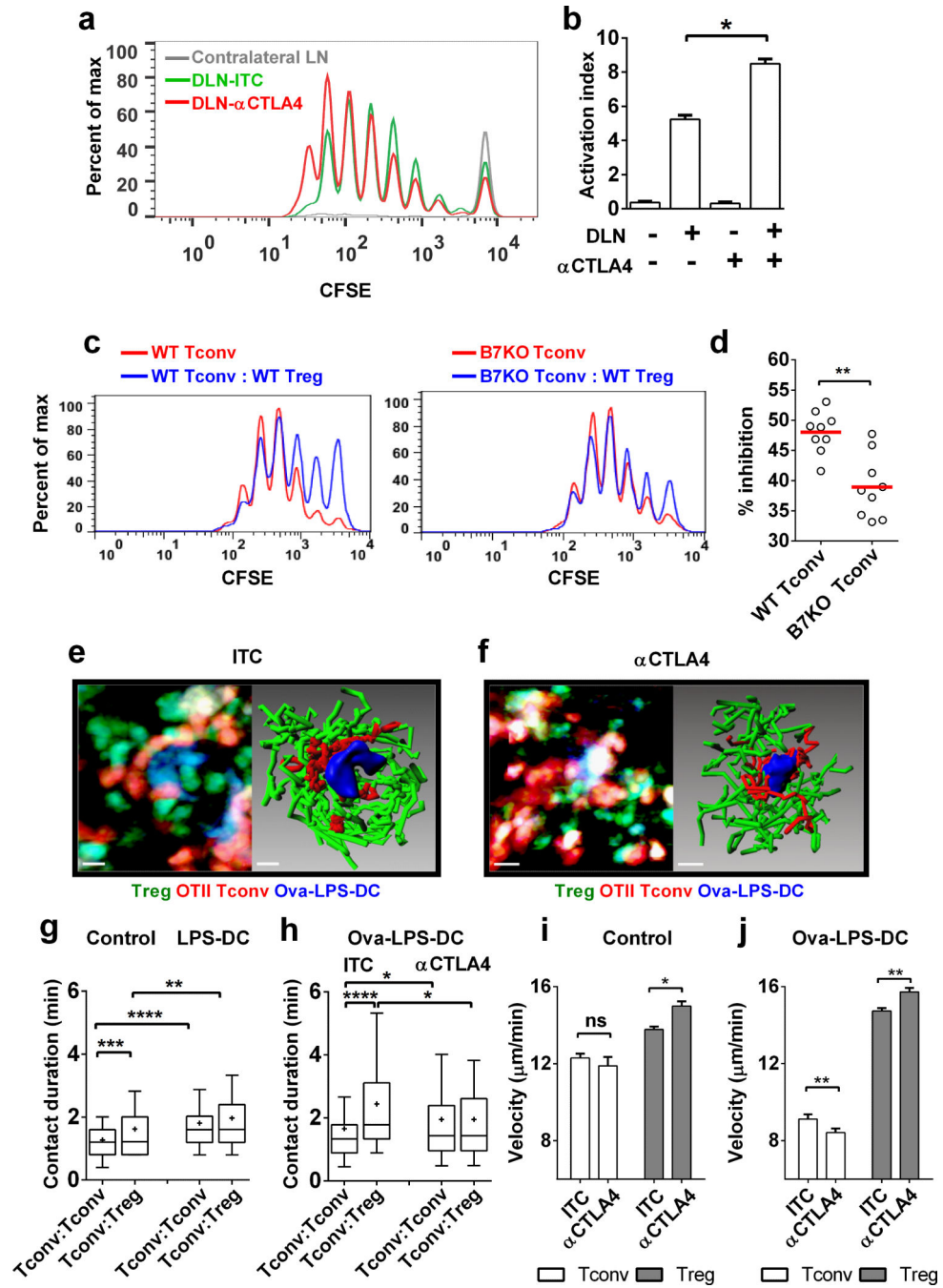


**Figure 6.**

CTLA4 is critical for Tconv-Treg interactions during priming. **(a)** CFSE dilution in OT-II Tconv cells 72 hr following transfer into WT mice primed with Ova-LPS pulsed DCs. Green and red lines for draining lymph node (DLN) of ITC- and  $\alpha$ CTLA4-treated mice, respectively; grey line for contralateral LN with  $\alpha$ CTLA4. **(b)** In vivo proliferation of OTII Tconv determined by CFSE dilution; data from 4-5 mice with  $\alpha$ CTLA4 or ITC control treatment. **(c)** In vitro proliferation of Tconv (WT, left, and B7-KO, right) after stimulation with anti-CD3/28 Dynabeads with (blue) and without (red) WT Treg co-culture (1:1 ratio).



(d) Inhibition of WT and B7-KO Tconv cell proliferation by WT Tregs; red bars indicate mean values, data pooled from two independent experiments. (e) Left: Ova-pulsed DCs (blue) interacting with OTII Tconvs (red) and Tregs (green) in a  $Foxp3^{EGFP}$  mouse. Right: tracks of Tconvs and Tregs that touched a DC at least once during imaging (20:55, min:sec); tracks normalized to DC position; scale bar = 10  $\mu\text{m}$ . (f) Left: Ova-pulsed DCs (blue), OTII Tconvs (red), and Tregs (green) in  $Foxp3^{EGFP}$  mouse treated with  $\alpha\text{CTLA4}$ . Right: tracks of Tconvs and Tregs that interacted with a DC (blue) at least once during imaging (20:33, min:sec). Scale bar = 10  $\mu\text{m}$ . (g) Contact durations of OTII Tconvs in the absence and presence of LPS-DCs. Basal: Tconv:Tconv, n = 135; Tconv:Treg, n = 234. LPS-DCs present: Tconv:Tconv, n = 108; Tconv:Treg, n = 145. (h) Contact durations of OTII Tconvs in the presence of Ova-pulsed DCs after treatment with 150  $\mu\text{g}$  isotype control (ITC) or  $\alpha\text{CTLA4}$  antibodies. ITC-treated: Tconv:Tconv, n = 101; Tconv:Treg, n = 108.  $\alpha\text{CTLA4}$ -treated: Tconv:Tconv, n = 87; Tconv:Treg, n = 152. (i) Velocities of OTII Tconvs and Tregs under basal conditions after treatment with ITC or  $\alpha\text{CTLA4}$  antibodies. Tconv tracks: n = 268 (ITC) and 238 ( $\alpha\text{CTLA4}$ ); Treg tracks: n = 296 (ITC) and 213 ( $\alpha\text{CTLA4}$ ). (j) Velocities of OTII Tconvs and Tregs in Ova-LPS-DC immunized mice after treatment with ITC or  $\alpha\text{CTLA4}$  antibodies. Tconv tracks: n = 99 (ITC) and 114 ( $\alpha\text{CTLA4}$ ). Treg tracks: n = 811 (ITC) and 305 ( $\alpha\text{CTLA4}$ ).

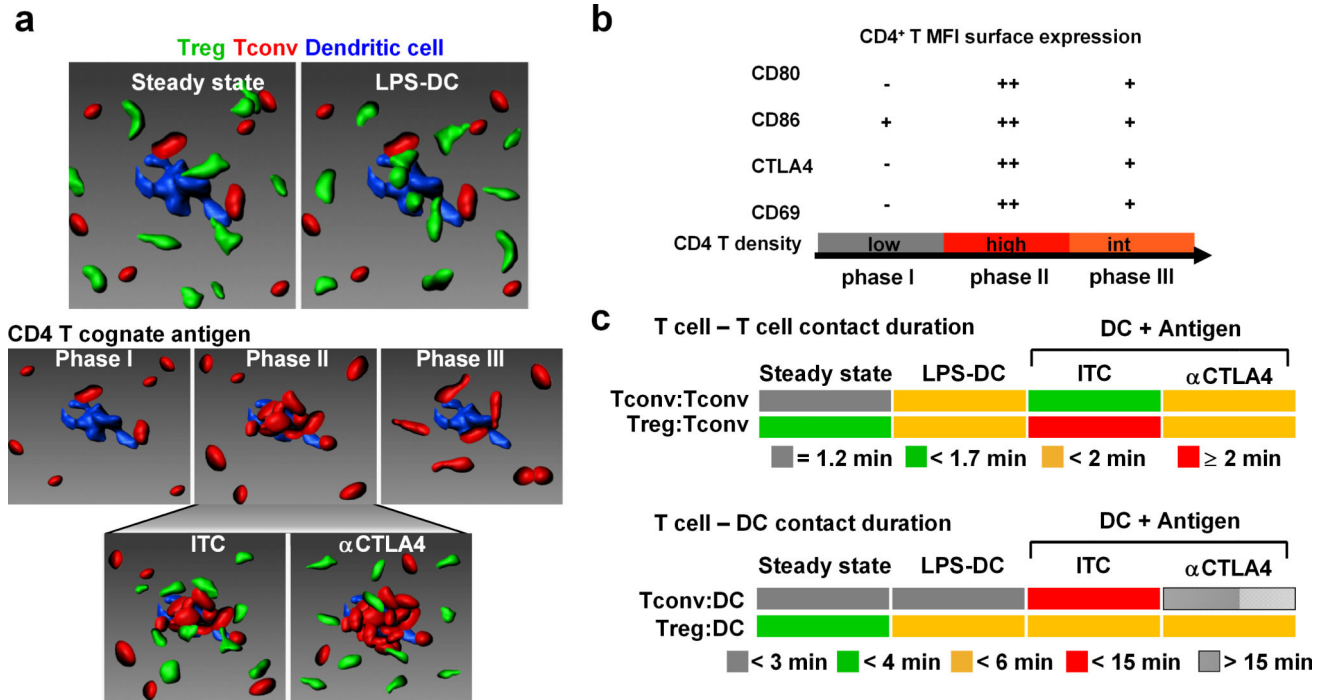


**Figure 7.** Summary of Treg, Tconv, and DC dynamics. **(a)** Cellular choreography illustrating cell dynamics and the role of CTLA using cell shapes rendered from 2P images (Tregs, green; Tconv, red; DCs, blue). Panels represent steady-state conditions (top left); inflammation (LPS DC; top right); T cell priming in three phases (middle); Tregs interacting with clusters during phase II under normal priming conditions (labeled ITC for isotype control; bottom left) and in the presence of CTLA4-blocking antibody (labeled αCTLA4; bottom right). **(b)** Chart of relative surface expression by Tconv cells during T cell priming. CD4 density refers to the local concentration of antigen-specific T cells near antigen-presenting DCs during phase 2. **(c)** Color-coded diagram of measured contact durations among Tregs and Tconvs (top panel), and among T cells and DCs (bottom panel). Each change in contact duration (different colors) represents a significant difference of at least  $p < 0.05$ .